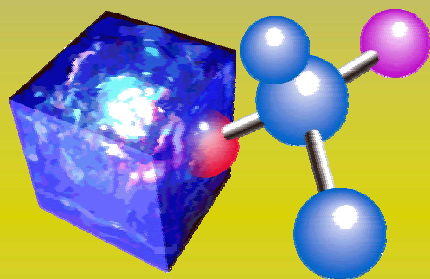
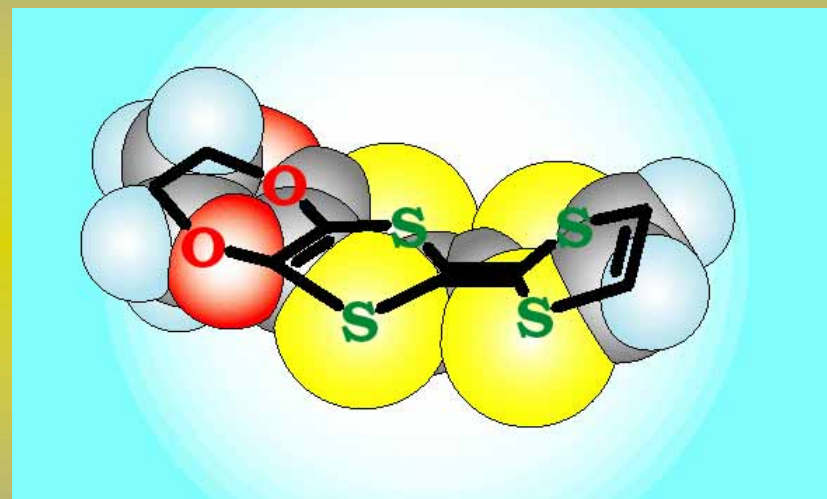


有機導電体における 分子自由度



低温物質科学
研究センター
矢持 秀起

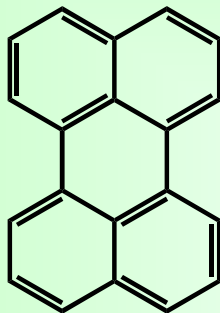


- 分子性導体の歴史
- (EDO-TTF)₂PF₆の多重不安定性
超高速・高効率光誘起相転移
- 分子の化学修飾と錯体の物性変化

Molecular Conductor

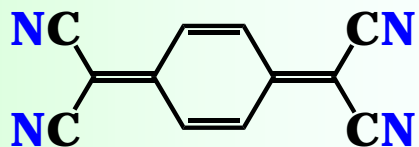
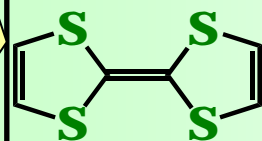
Summarized History

1954 Organic Semiconductor



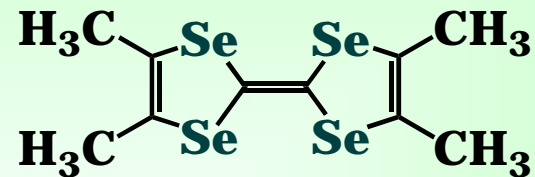
• Br₂

1960s 1D Organic Metals

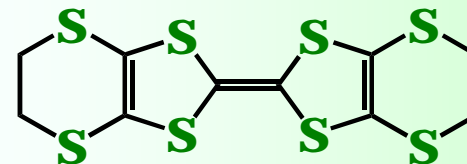


Increment of Dimensionality

1980s: Organic Superconductors



Q1D Superconductors
max. $T_c = 1.4$ K (AP)



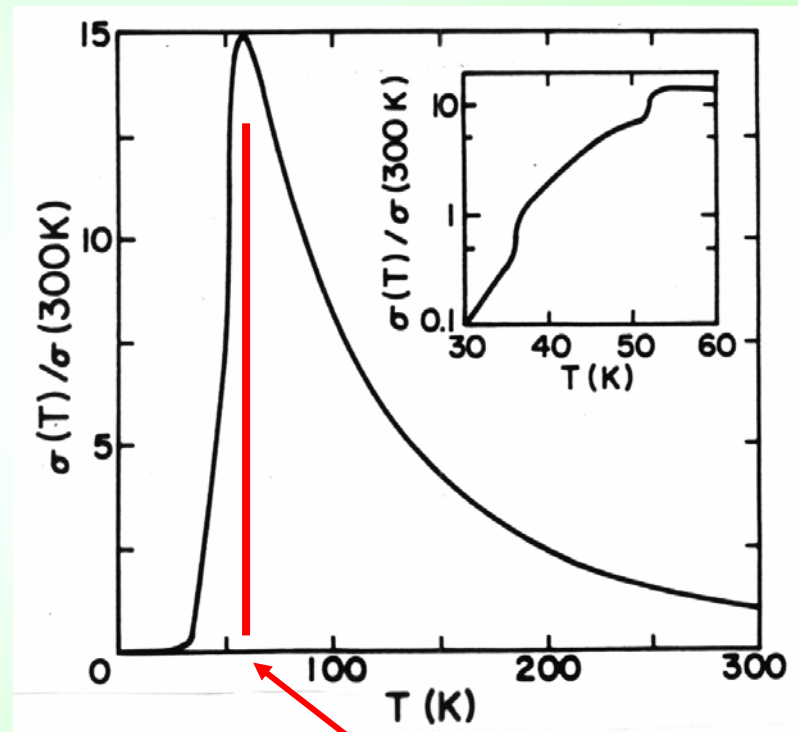
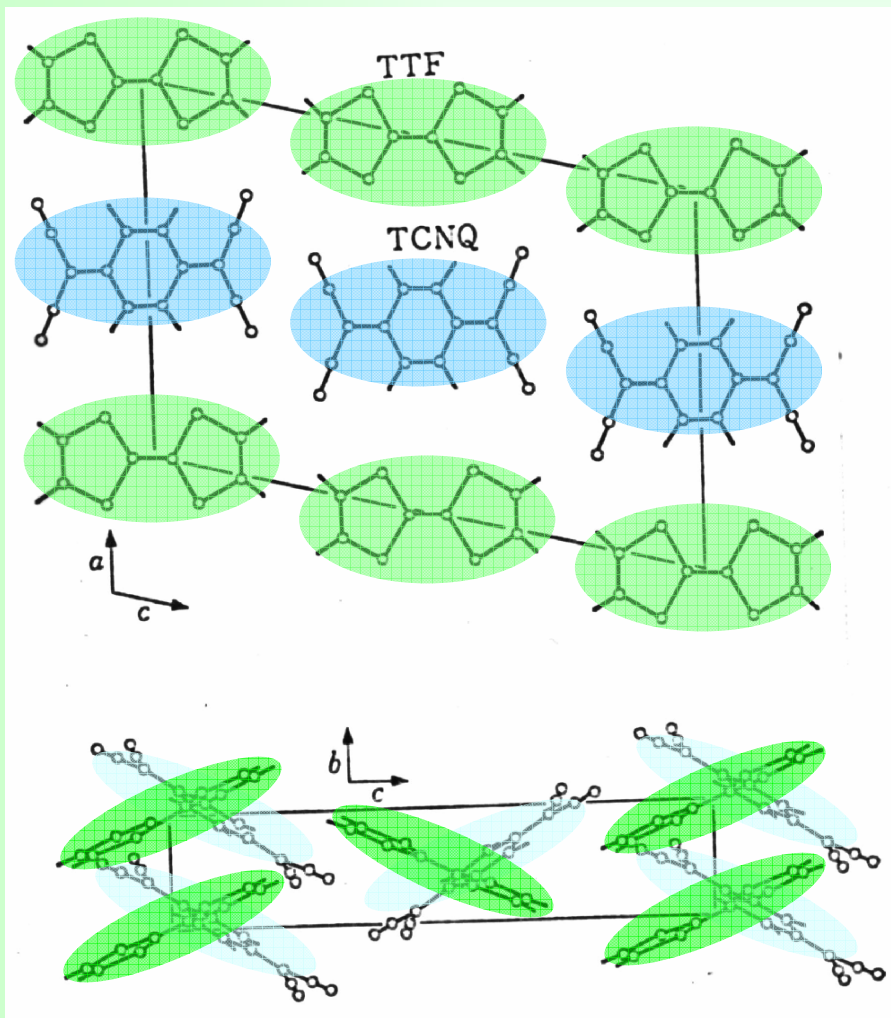
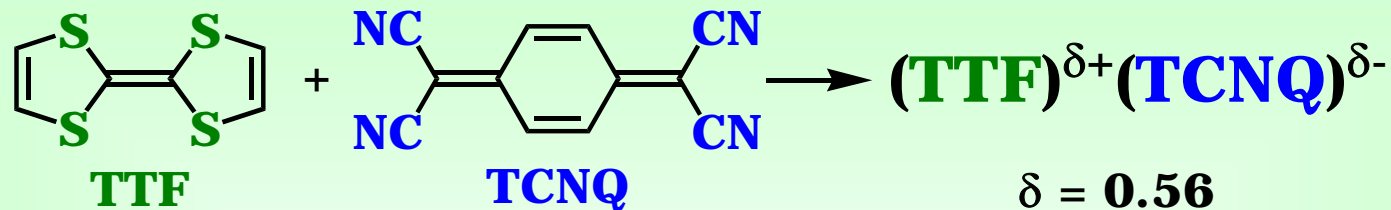
2D Superconductors
max. $T_c = 12.3$ K (AP)

1990s: 3D Molecular Superconductors



max. $T_c = 33$ K (AP)

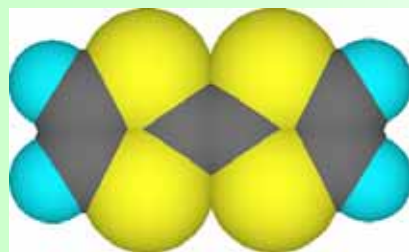
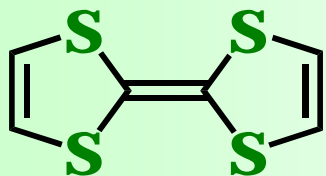
TTF•TCNQ - The First Organic Metal



38 K **54 K**
Peierls gap **Peierls gap**
In TTF chain **in TCNQ chain**
Semiconductor **Metal**

Increasing the Dimensionality

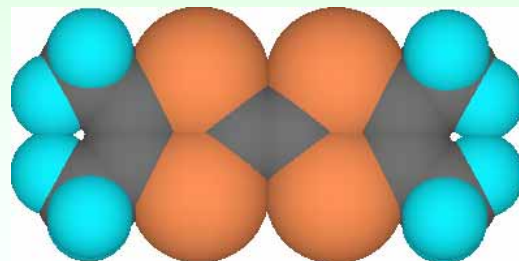
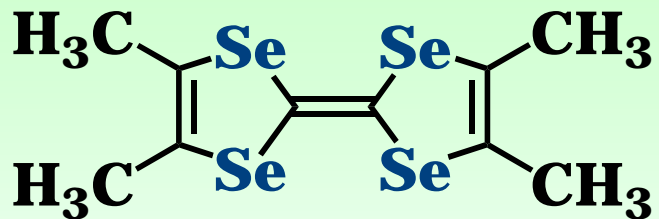
Increment of side-by-side intermolecular interaction



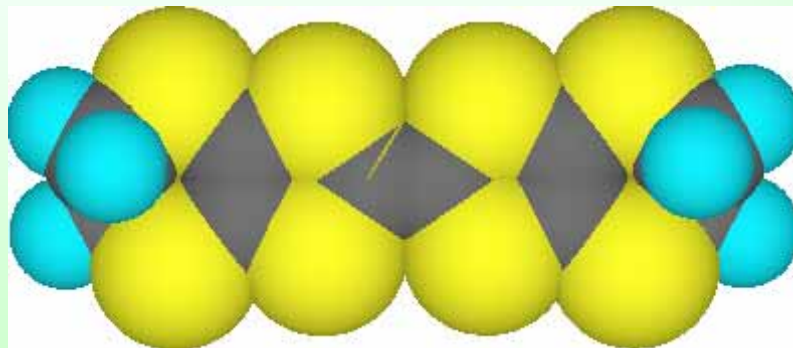
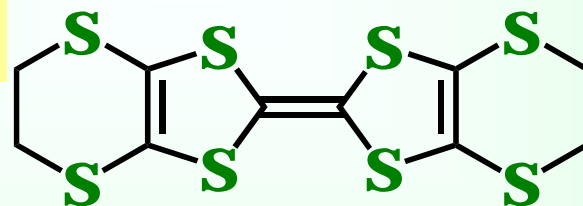
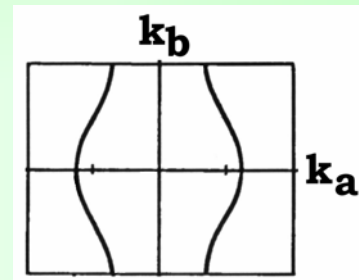
TTF

Atom Size

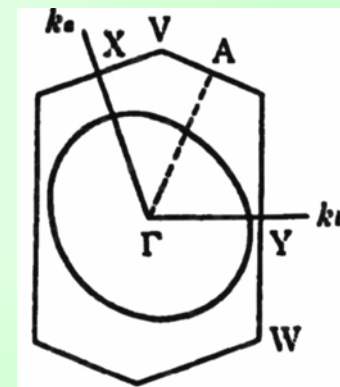
Number of Atoms



TMTSF

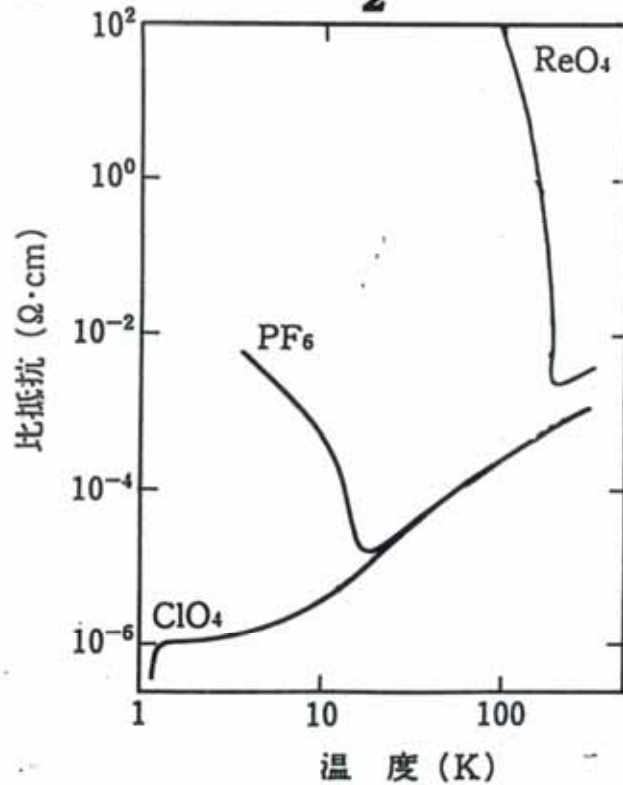
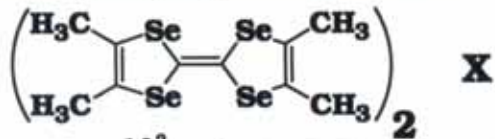


BEDT-TTF (ET)

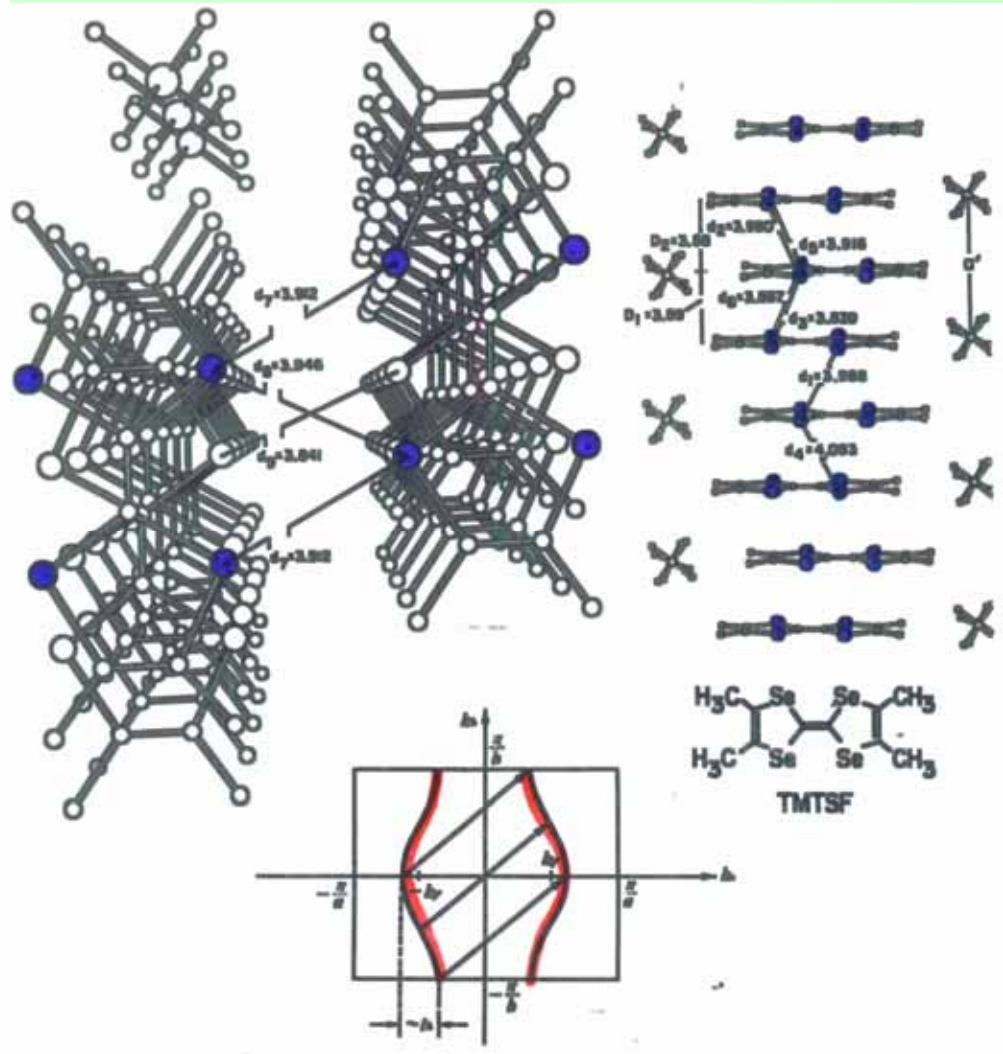


TMTSF Superconductors

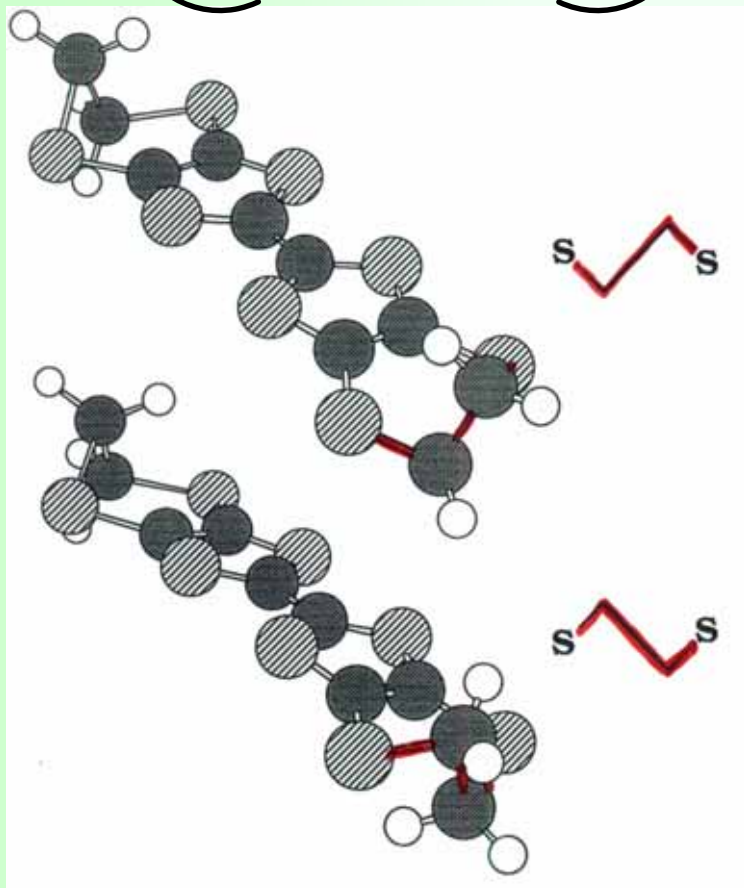
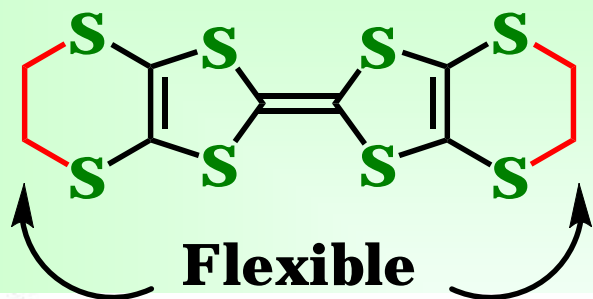
TMTSF (Super)conductors



Compound	T_c (K)	Pressure (Kbar)
PF_6^-	0.9	10-12
ClO_4^-	1.2	none
ReO_4^-	1.3 - 1.5	12
FSO_3^-	2.5	>6



BEDT-TTF Superconductors

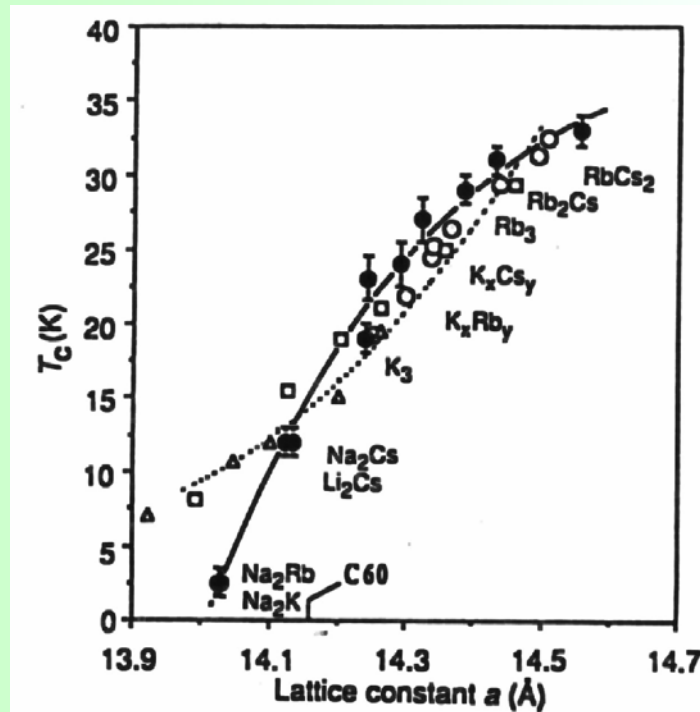
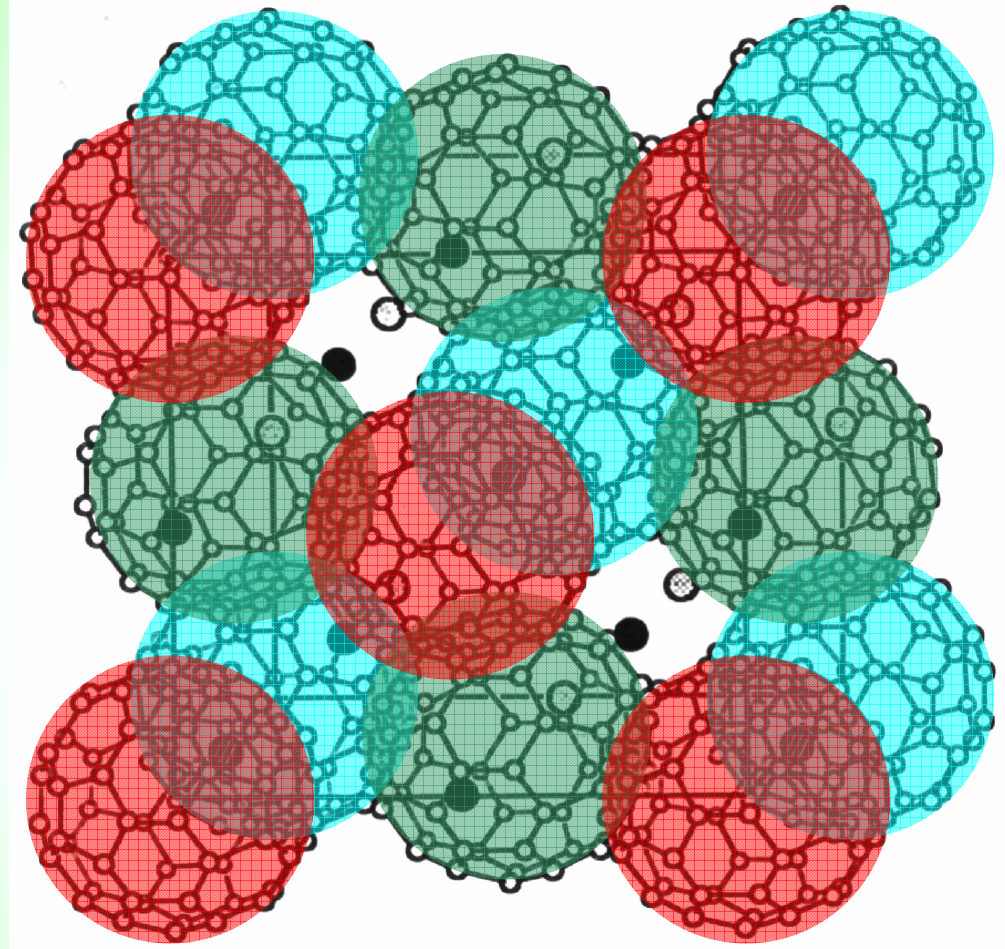


BEDT-TTF(ET) Ambient Pressure Superconductors (Planar Anion Layers)

T_c	Complex
11.8 K	κ -(ET) ₂ Cu[N(CN) ₂]Br
11.2 K	κ -(ET) ₂ Cu(CN)[N(CN) ₂]
11.1 K	κ_H -(ET) ₂ Ag(CF ₃) ₄ (TCE) (11.1 & 9.4 K)
10.5 K	κ_H -(ET) ₂ Au(CF ₃) ₄ (TCE)
10.4 K	κ -(ET) ₂ Cu(NCS) ₂
10.2 K	κ_H -(ET) ₂ Ag(CF ₃) ₄ (CHCl ₂ -CH ₂ Br)
9.2 K	κ_H -(ET) ₂ Cu(CF ₃) ₄ (TCE) _x (x < 1)
8.5 K	β'' -(ET) ₄ [(H ₂ O)Fe(ox) ₃](PhCN)
8.1 K	β_H -(ET) ₂ I ₃
5.2 K	κ_L -(ET) ₂ Cu(CF ₃) ₄ (CHBr ₂ -CH ₂ Br)
5.0 K	κ -(ET) ₂ Ag(CN) ₂ H ₂ O
5.0 K	β -(ET) ₂ AuI ₂
4.9 K	κ_L -(ET) ₂ Cu(CF ₃) ₄ (CHCl ₂ -CH ₂ Br)
4.8 K	κ_L -(ET) ₂ Ag(CF ₃) ₄ (CHBr ₂ -CH ₂ Br)
4.5 K	κ_L -(ET) ₂ Ag(CF ₃) ₄ (CHBrCl-CH ₂ Br)
4.1 K	κ_L -(ET) ₂ Ag(CF ₃) ₄ (CHCl ₂ -CH ₂ Br)
4.0 K	κ_L -(ET) ₂ Cu(CF ₃) ₄ (TCE)
3.8 K	κ_L -(ET) ₂ Ag(CF ₃) ₄ (CHBrCl-CH ₂ Cl)
3.8 K	κ' -(ET) ₂ Cu ₂ (CN) ₃
3.6 K	κ -(ET) ₂ I ₃
3.6 K	θ -(ET) ₂ I ₃
2.7 K	β -(ET) ₂ IBr ₂
2.6 K	κ_L -(ET) ₂ Ag(CF ₃) ₄ (TCE)
2.1 K	κ_L -(ET) ₂ Au(CF ₃) ₄ (TCE)
1.5 K	β_L (ET) ₂ I ₃
0.8 K	α -(ET) ₂ NH ₄ Hg(SCN) ₄
0.3 K	α -(ET) ₂ KHg(SCN) ₄

**& much more
at present**

3-dimensional Superconductors

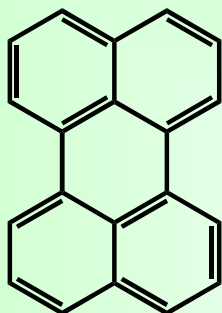


Alkali metals are in the interstitial sites among C_{60} 's.

Max $T_c = 33$ K ($\text{RbCs}_2\text{C}_{60}$)

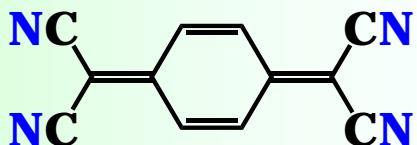
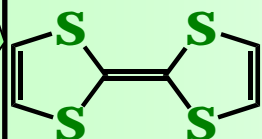
Summarized History

1954 Organic Semiconductor



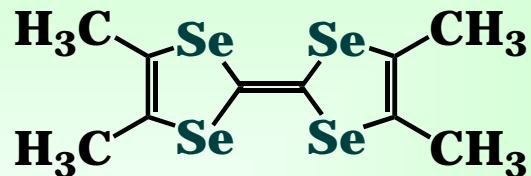
• Br₂

1960s 1D Organic Metals

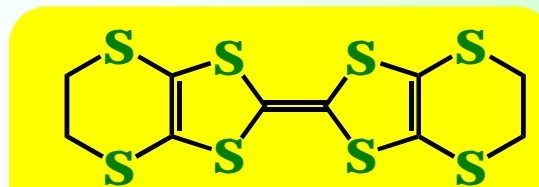


Increment of Dimensionality

1980s: Organic Superconductors



Q1D Superconductors
max. $T_c = 1.4$ K (AP)

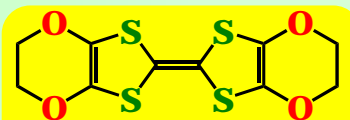


2D Superconductors
max. $T_c = 12.3$ K (AP)

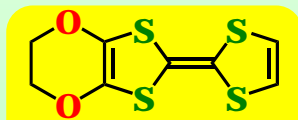
Molecular Degree of Freedom

Lattice point \neq Simply a point

- ✓ Size
- ✓ Shape
- ✓ Functionality



BEDO-TTF (BO)



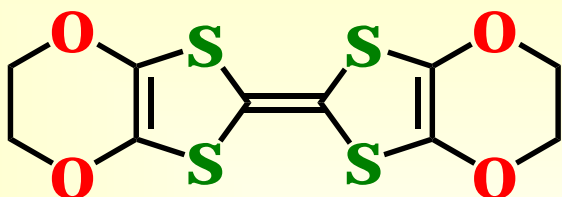
EDO-TTF

1990s: 3D Molecular Superconductors

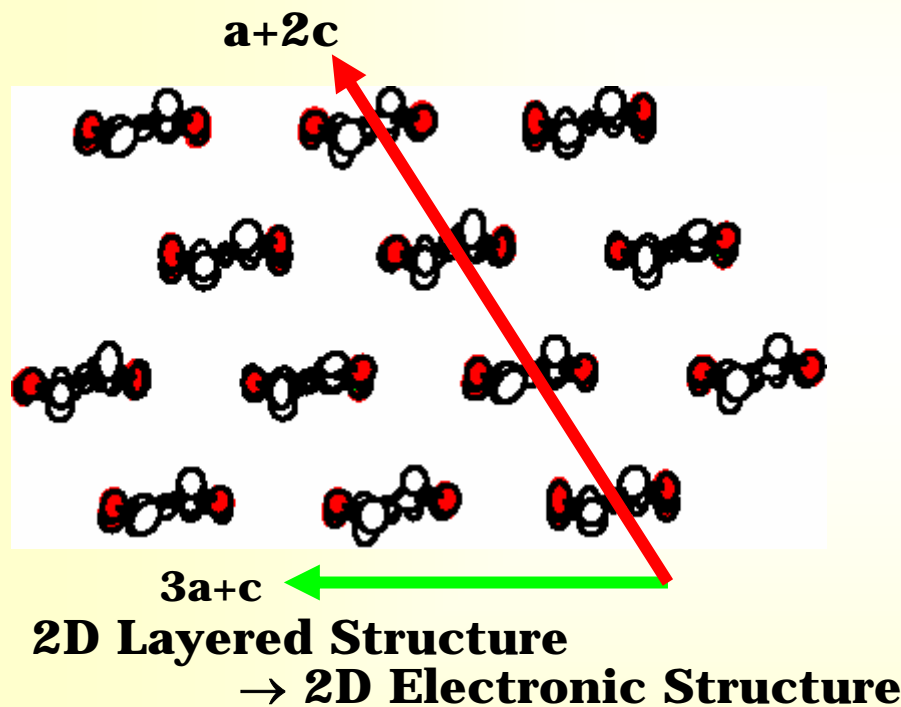


max. $T_c = 33$ K (AP)

BEDO-TTF(BO) Salt



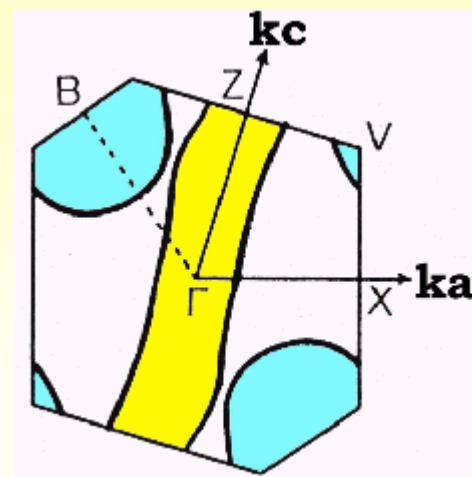
Self-assembling Packing Pattern



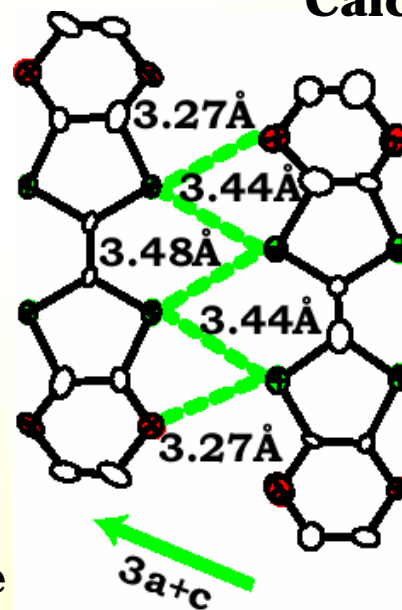
Side-by-side

Heteroatomic Contacts

Weak Hydrogen Bond Network



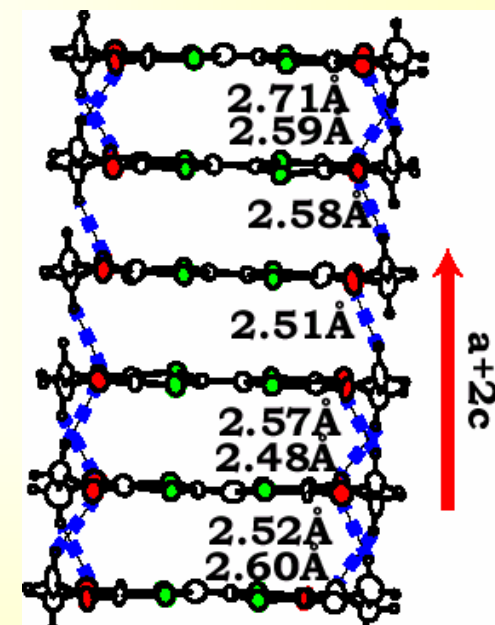
Calculated Fermi Surface



vdW

$S \cdots S = 3.60 \text{ \AA}$

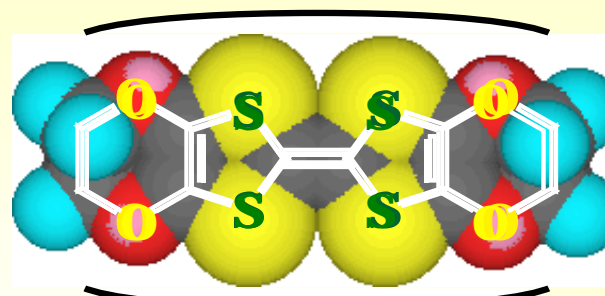
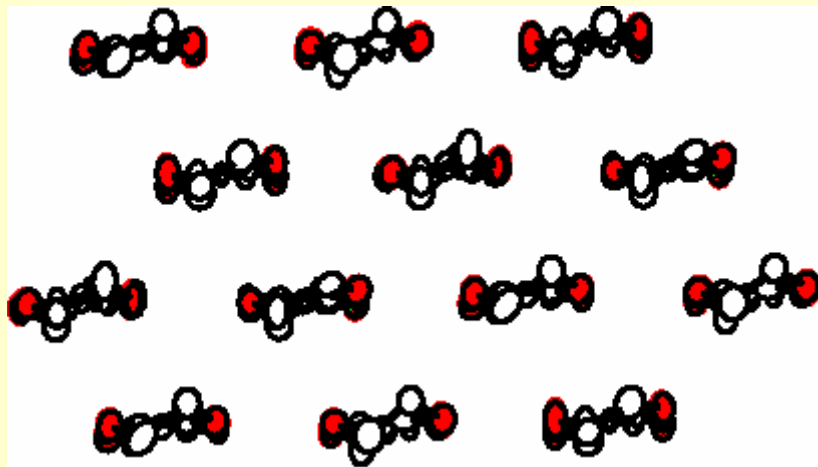
$S \cdots O = 3.32 \text{ \AA}$



vdW

$H \cdots O = 2.72 \text{ \AA}$

Partial Suppression of Self-assembling Nature of BO



Flat Side Surface

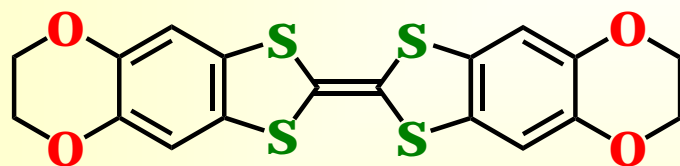
-OCH₂CH₂O-

→ Stable Metal

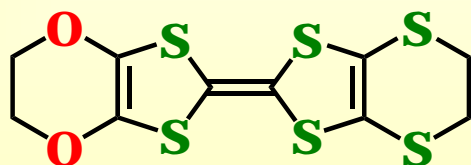
NO PHASE TRANSITION

obstruction

Introduction of
Bulky Substituent

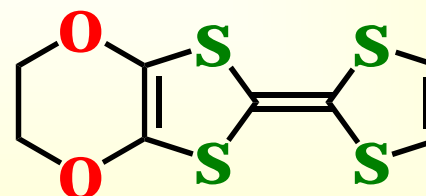


BEDO-DBTTF



EOET

Removal of an
EDO Group

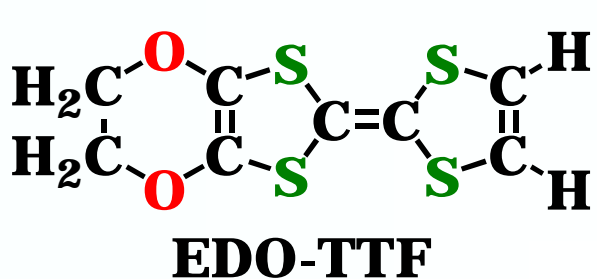


EDO-TTF



EDO-TTF Complexes

At 2001 (when we started): Synthesis of donor
A few kinds of complexes: No description of composition
Conductivity: No description or $\leq 2 \times 10^{-4} \text{ Scm}^{-1}$



+ TCNQ deriv. → **No Metal**
No Self-assembling

A. Ota, et al., *Mol. Cryst. Liq. Cryst.*, **376**, 177-182 (2002)

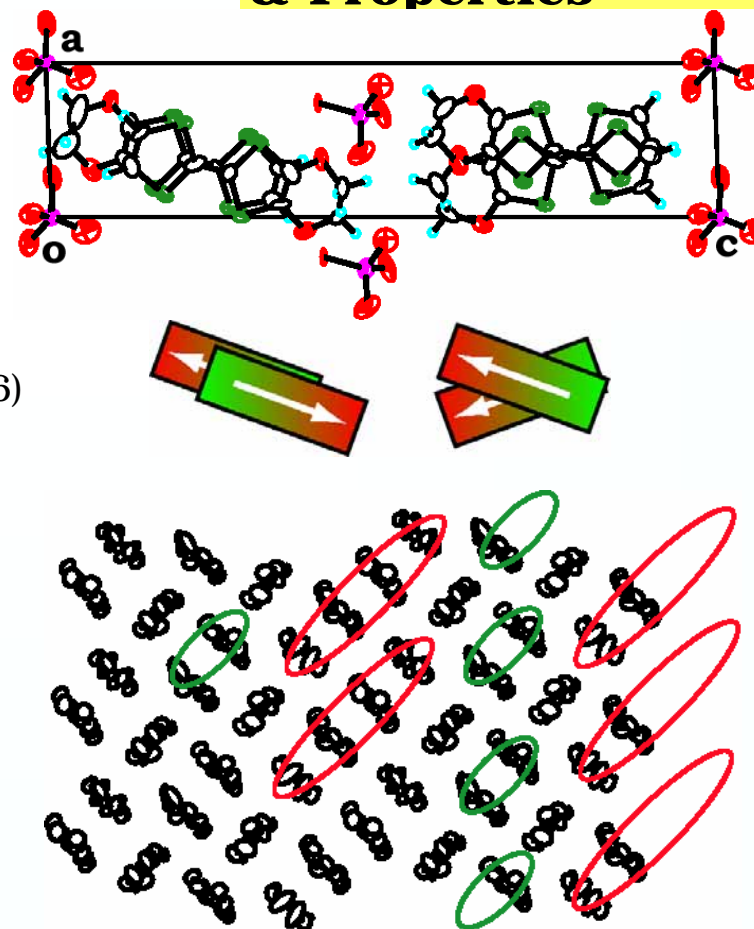
+ Inorg. Anions → **Variety of Structure & Properties**

2:1 ReO_4 , GaCl_4
 $\sigma_{\text{RT}} = 130, 54 \text{ Scm}^{-1}$
Activated behaviors $\leq 250 \text{ K}$
Different typed columns

A. Ota et al., *J. Low Temp. Phys.*, **142**(3/4), 425 (2006)

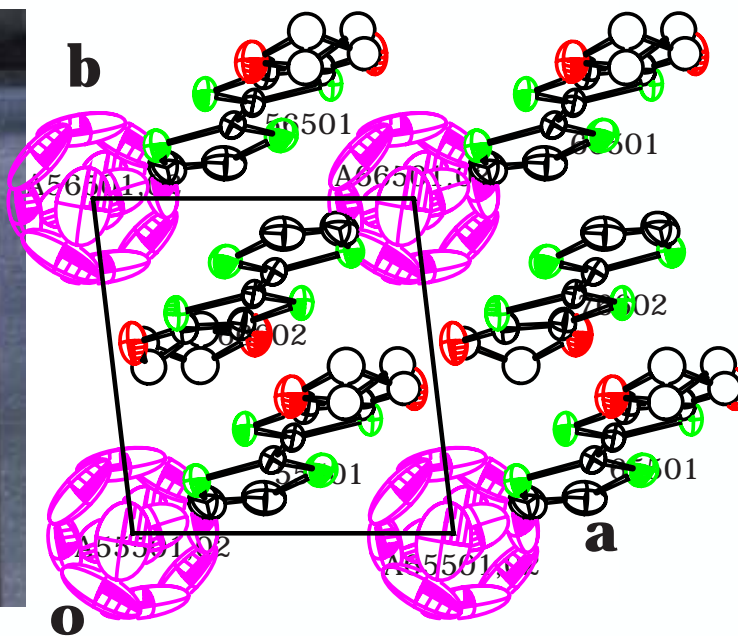
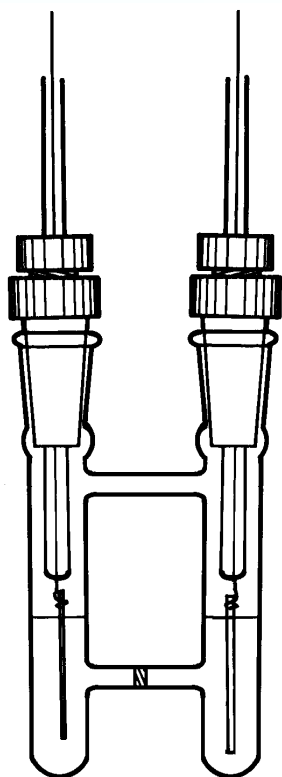
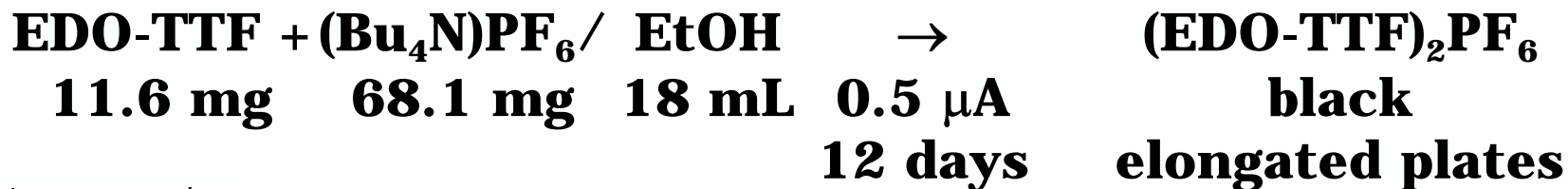
5:3 BF_4
 $\sigma_{\text{RT}} = 1 \text{ Scm}^{-1}$ ($E_a = 62 \text{ meV}$)
4:0.85:4(H_2O) Sb_2F_{11}
 $\sigma_{\text{RT}} = 2 \text{ Scm}^{-1}$ ($E_a = 55 \text{ meV}$)
Multimer & monomer

A. Ota et al., in "Multifunctional Conducting Molecular Materials", eds. G. Saito et al., RSC Publishing, Cambridge, UK. (2007), pp. 115-118.

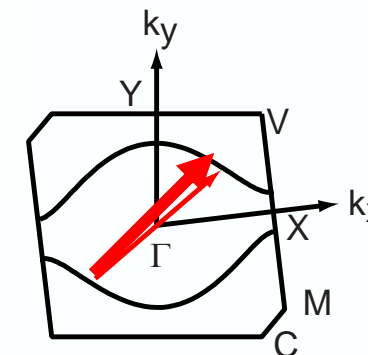


EDO-TTF — Preparation of PF₆ Complex

Electrooxidation (Electrocrystallization)



Triclinic P 1
 a = 7.197(0.9) Å
 b = 7.343(0.6)
 c = 11.948(1)
 α = 93.454(7)°
 β = 75.158(6)
 γ = 97.405(7)
 V = 605.0(1) Å³
 Z = 1
 R = 5.6 %

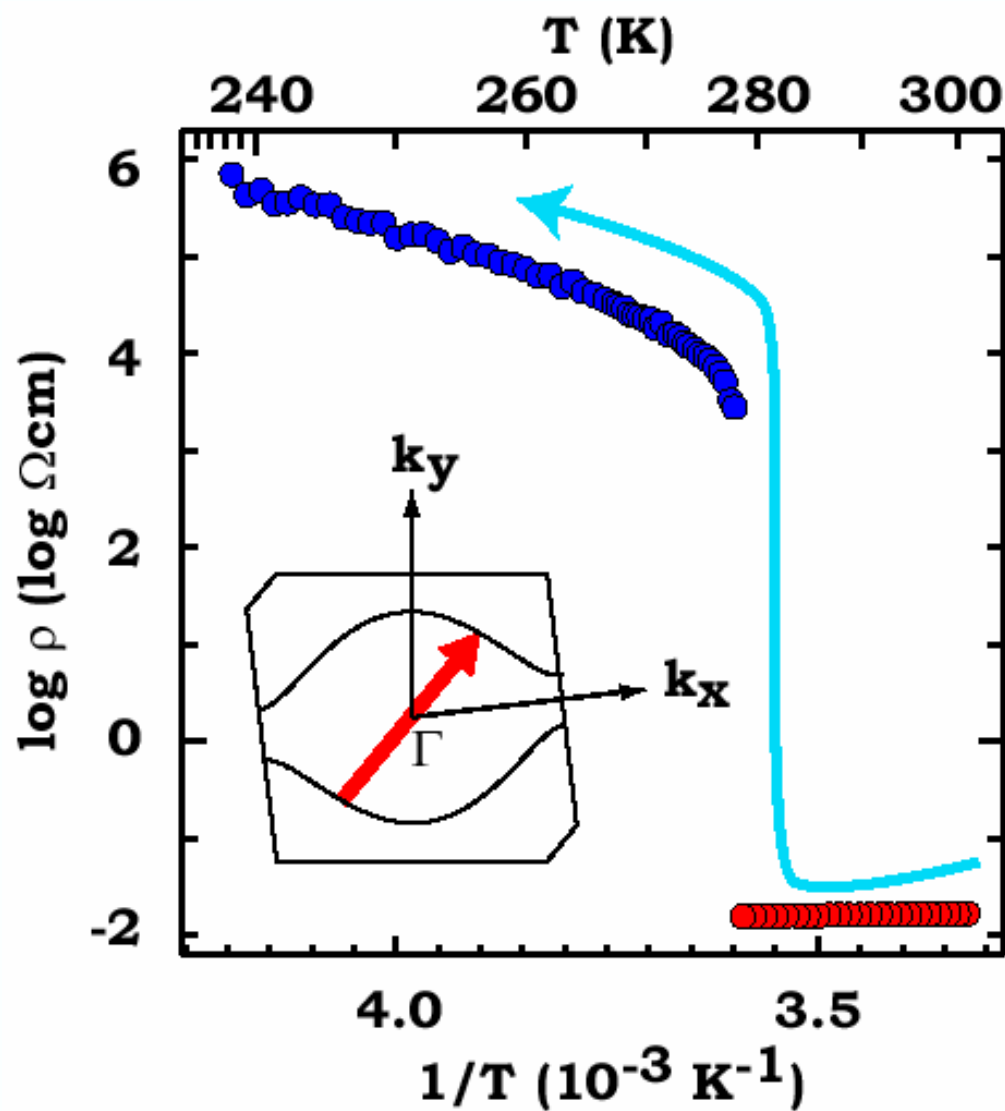


EDO-TTF was added to (+)
 side only, while ca. half
 amount of (Bu₄N)PF₆ was
 added to each chamber.

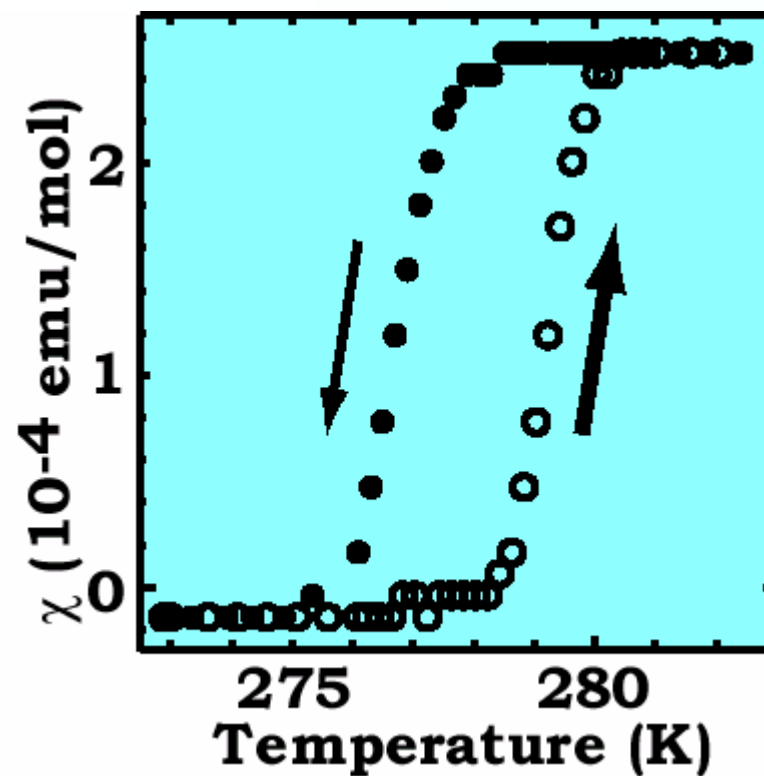
Head-to-Tail Stacking along b-axis.
Disordered Ethylene.
Isotropic Rotation of PF₆⁻.

Almost Uniform 1D Intermolecular Overlap Integrals.

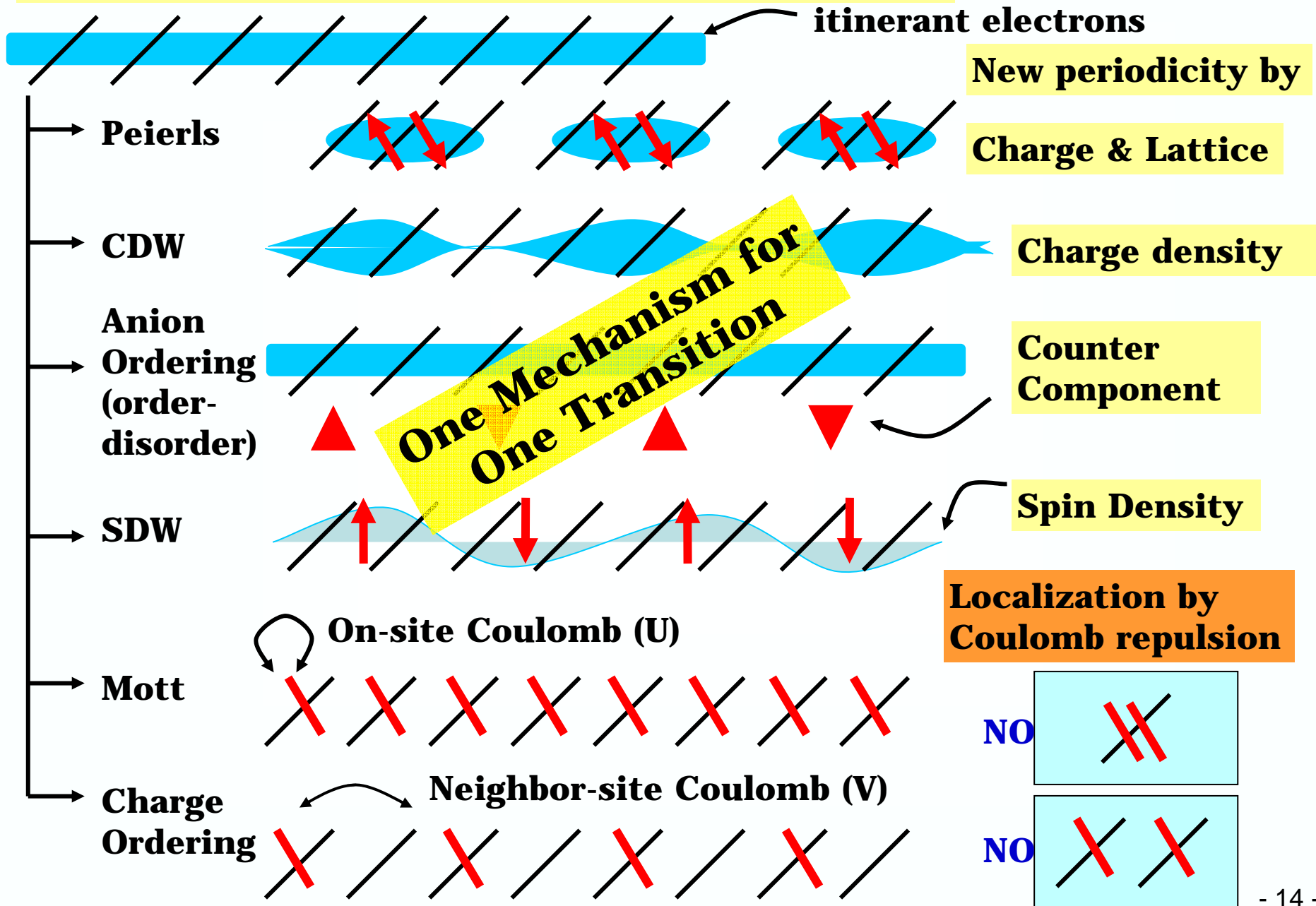
Thermally Induced MI Transition of $(\text{EDO-TTF})_2\text{PF}_6$



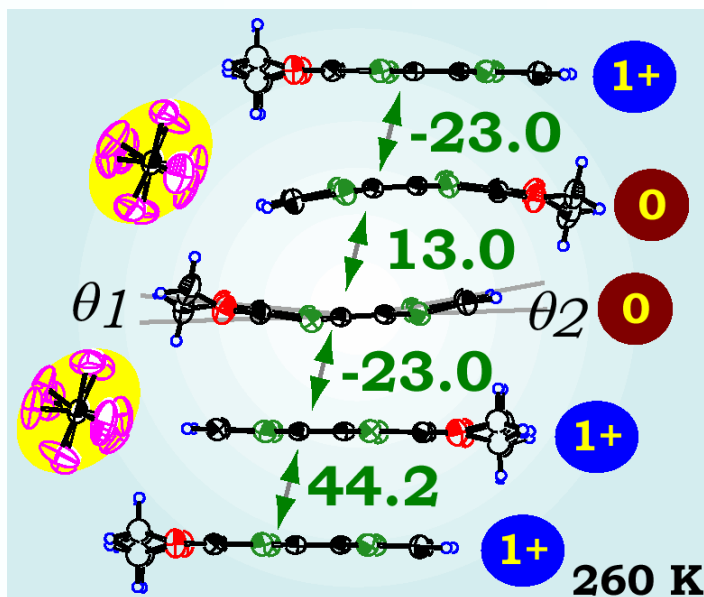
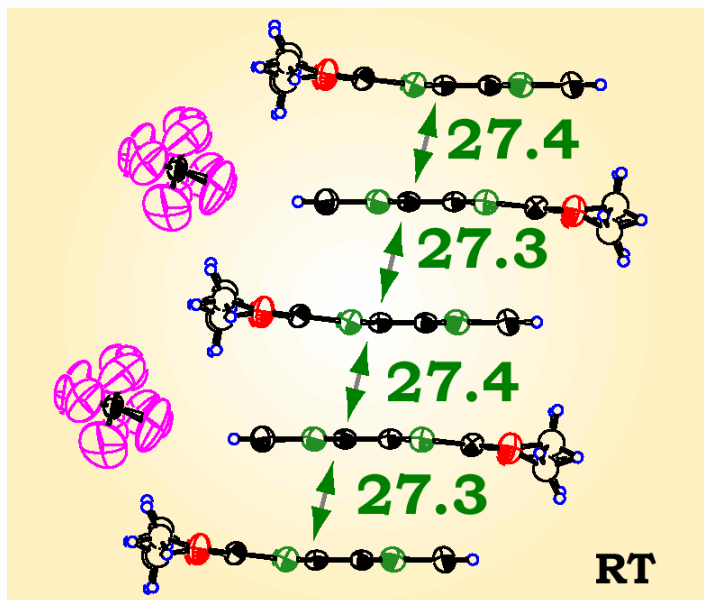
$T_{\text{MI}} \approx 280 \text{ K}$
 ρ jump: ca. 5 order
Paramag. \leftrightarrow Non-mag.
First-order Transition



How Metal-Insulator Transitions Occur



(EDO-TTF)₂PF₆ — Above and Below T_{MI} (280 K)



(Overlap Integral × 10³)

Distinct Molecular Deformation

$\theta_1, \theta_2:$
6.0°, 0.3°

planar: 0.8°, 2.1°
bent: 11.1°, 7.9°

**Overlap
Integral**

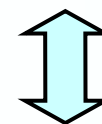
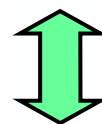
Uniform

**from
Bond
Length**

0.5+

**PF₆
Rotation**

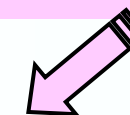
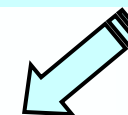
Isotropic



Alternate

1+/0

Uniaxial



Peierls

**Charge
Ordering**

**Order-
Disorder**

Molecular Deformation is regarded as the Origin to Mix Metal-Insulator Transition Mechanisms (Multi-instability).

(EDO-TTF)₂PF₆ – Other Properties –



Raman Spectra: 4.2 K → Coexistence of 0.9+, 0.1+ Donors

O. Drozdova et al., *Synthetic Metals*, **133-134**, 277-279 (2003).



Accurate Structure Analysis with MEM method:

285 K → +0.6(1)

260 K → F: +0.8(1) , B: +0.2(1)

S. Aoyagi et al., *Angew. Chem. Int. Ed.*, **43(28)**, 3670-3673 (2004) .



Reflection Spectra: Significant Temperature Dependence

O. Drozdova et al., *Phys. Rev.*, **B70(7)**, 075107-1-8 (2004) .



Calorimetry: Transition Entropy

→ Unharmonicity of PF₆ Rotation in RT Phase

K. Saito et al., *Chem. Phys. Lett.*, **401(1-3)**, 76-79 (2005).



Uni-axial Strain: along c* → T_{MI}↑ (> 60 K/4 kbar)

M. Sakata et al., *Synthetic Metals*, **153(1-3)**, 393-396 (2005).

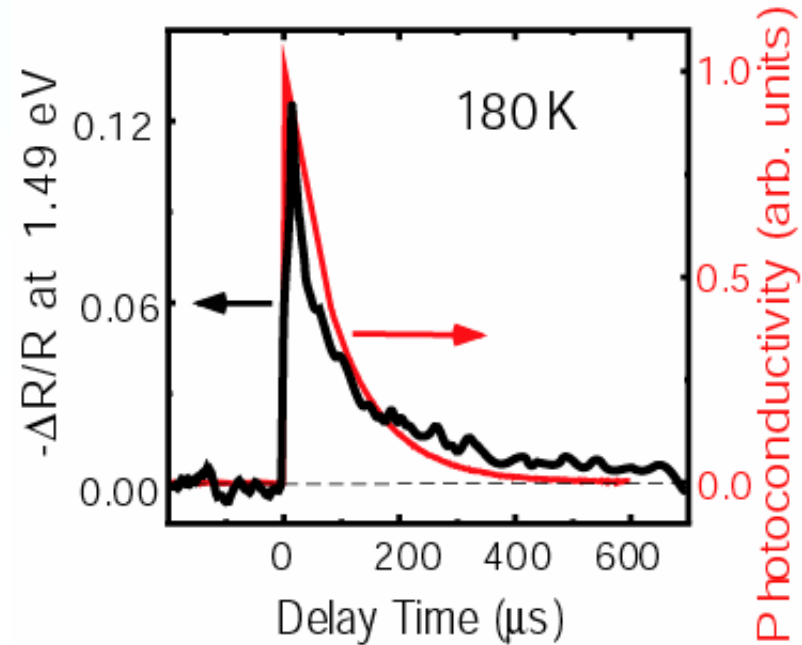
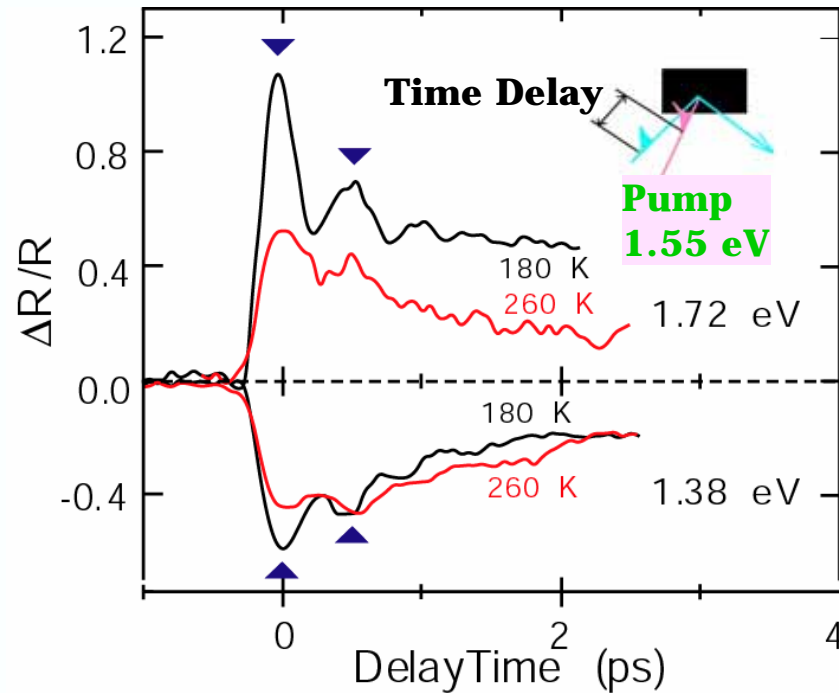


Photo-induced Phase Transition:

Ultra-fast Highly Efficient, ~ 0.1 ps, 50 - 500 donors/photon

M. Chollet et al., *Science*, **307**, 86-89 (2005).

Photo-induced Phase Transition (PIPT)



Completes in ca. 1.5 ps

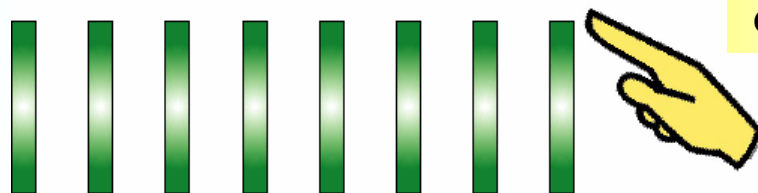
1 photon / 50-500 molecules

PIPT to Highly Conducting Metastable State

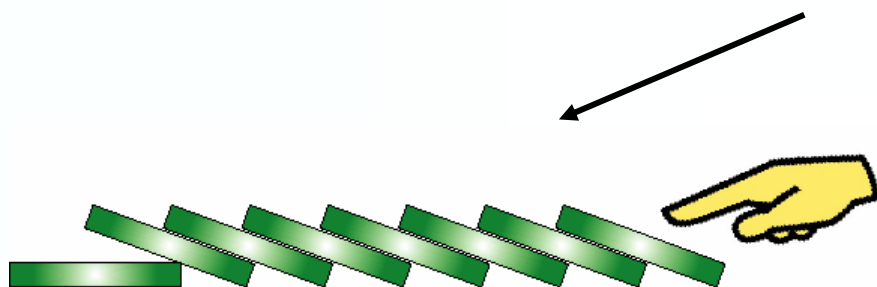
vibration: ca. 0.5 ps/cycle at 180 K

Strong Electron-Lattice Interaction

PIPT — Comparison with other systems

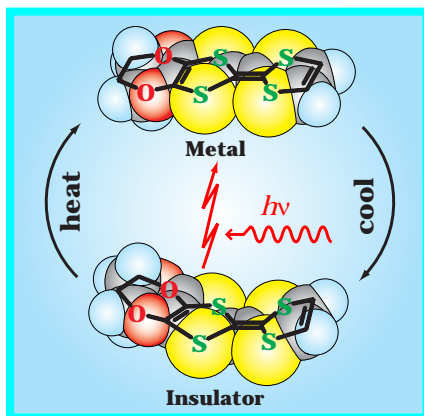


one photon



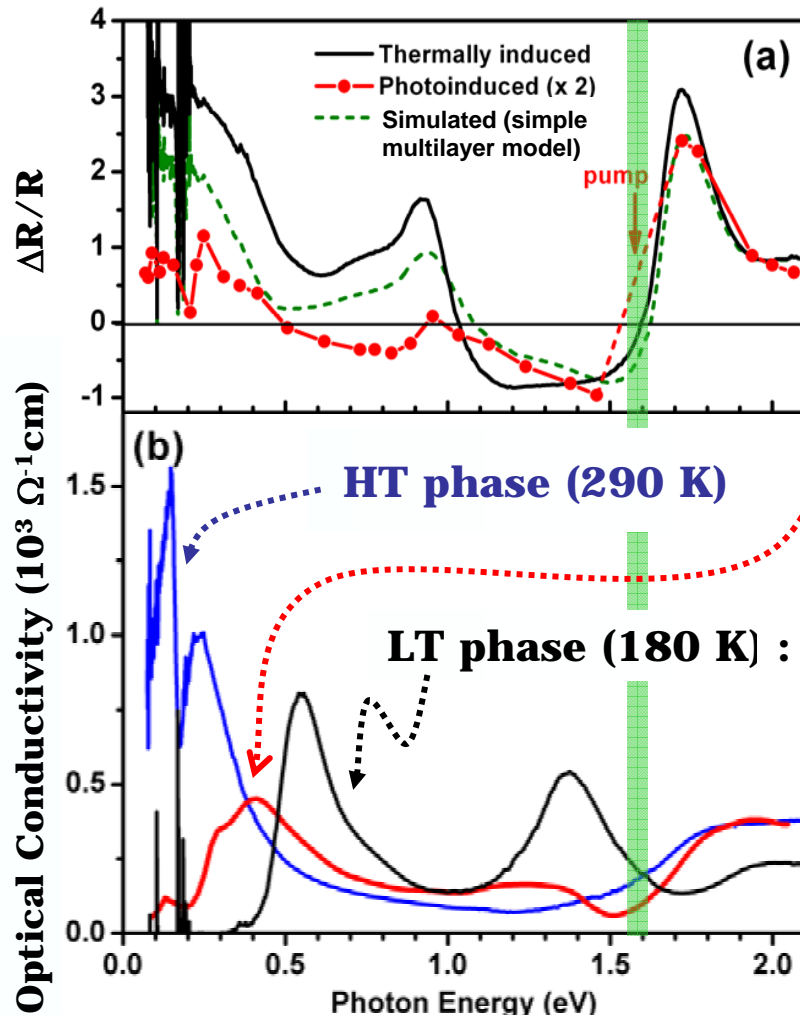
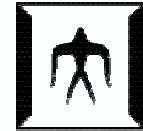
Our system
50 – 500 molecules
within ca. 0.1 ps

RbTCNQ (Ins. - Metal)
< 10 molecules, ca. 0.1 ps
TTF-Chloranil (Neutral - Ionic)
280-2,800 molecules, ~1 ns



Ultra-fast & Highly Efficient PIPT
Controllable Initialization
Development of Phase Transition
→ Dynamics of Non-equilibrium State

PI Metastable State \neq RT Metallic Phase



Wide Range Optical Conductivity Spectra

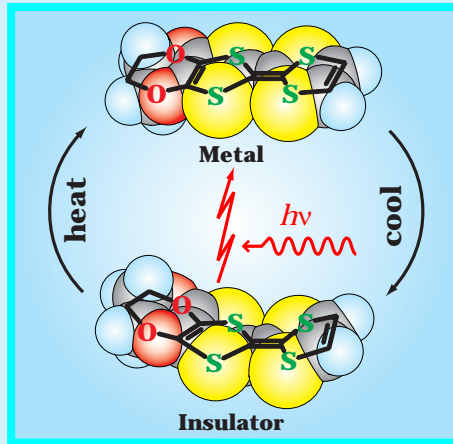
**0.1 ps after pump
one peak at low energy**

Theoretical Calculation
 $H: t, U, V, \gamma$ (e-ph coupling
 \ni anion potential modulation)
time dependent model

**PIPT state: (1010) Charge Disp.
 \neq RT Metallic ($\frac{1}{2} \frac{1}{2} \frac{1}{2} \frac{1}{2}$) Phase
 Lattice potential:
 fluctuated in this time scale**

K. Onda, S. Ogihara, K. Yonemitsu, N. Maeshima, T. Ishikawa, Y. Okimoto, X.F. Shao, Y. Nakano, H. Yamochi, G. Saito, S. Koshihara, *Phys. Rev. Lett.*, 101(6), 067403-1-4 (2008)

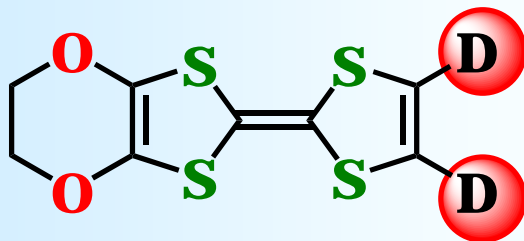
After (EDO-TTF)₂PF₆ – Isotope Effect



Electron-Phonon (Electron-Molecular Vibration) Coupling

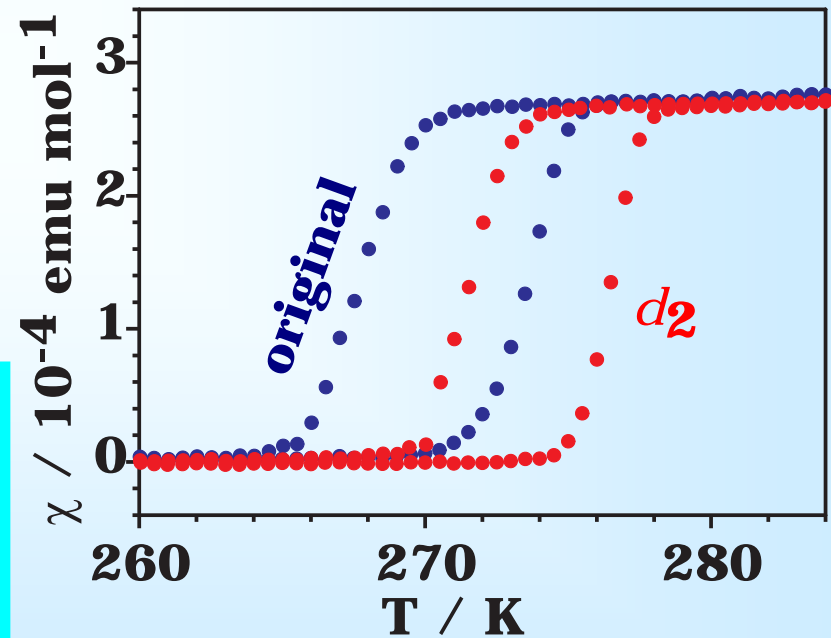


**Isotope substitution
→ Lattice (Molecular) Vibrations**



EDO-TTF-*d*₂

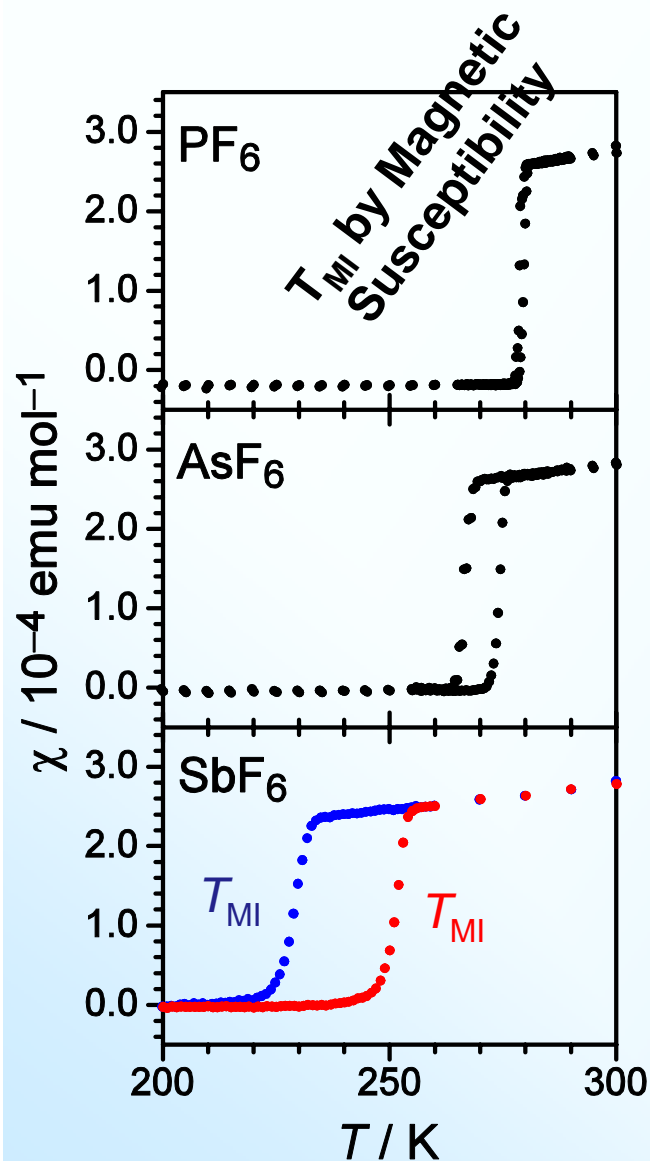
- **Modulation of π -system (conduction path) vibrations**
- **For PF₆ & AsF₆ complexes**
***d*₀ → *d*₂: $\Delta T_{MI} \approx 3$ K**



(EDO-TTF-*d*_x)₂AsF₆

After (EDO-TTF)₂PF₆ – Anion Size Effect

Isostructural (EDO-TTF)₂XF₆ (X = P, As Sb)

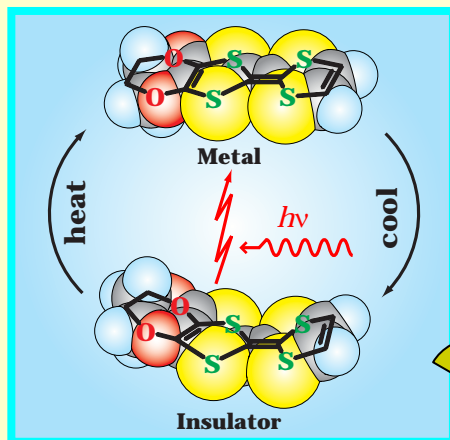


	Size	T_{MI} (K)	T_{MI} (K)
PF ₆	↓	279.0	1.0
AsF ₆	↓	270.8	5.5
SbF ₆	↓	242	14

スライド内容 一部削除

ここで観測された、転移温度とヒステリシス幅の陰イオン依存性については、現在、その詳細を解析中です。

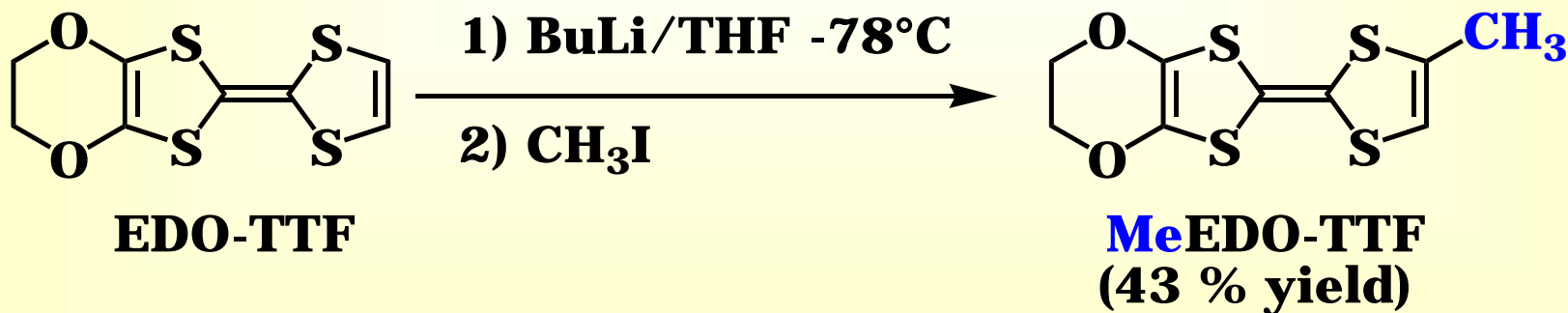
Molecular Design Based on EDO-TTF



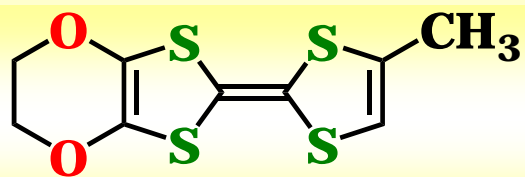
Distinct Molecular Deformation
Multi-instability of Itinerant Electrons

To Find Further Peculiar Systems
Similar π -electron system
Similar Molecular Size
Lower Symmetry

EDO-TTF having Small Sized Substituent



cf. 17 % yield: A. Miyazaki et al., (2001)

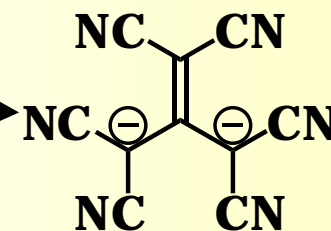


Complexes

MeEDO-TTF

Anion	D : A	σ_{rt} (S cm ⁻¹) Compressed Pellets
BF₄	2 : 1	26 (Metal)
ClO₄	2 : 1	24 (Metal)
PF₆	2 : 1	3 (Semi.)
AsF₆	2 : 1	15 (MI at 240 K)
SbF₆	2 : 1	6 (MI at 250 K)
HCTMM	4 : 1	6 (Semi.)

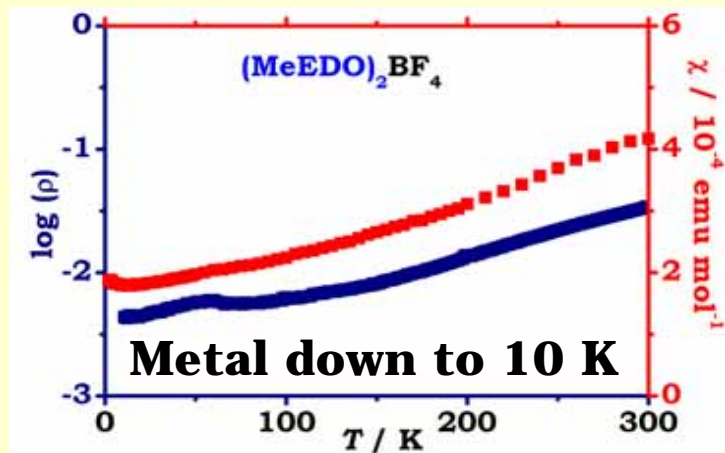
X.F. Shao et al., *J. Mater. Chem.*, **18**, 2131-2140 (2008)



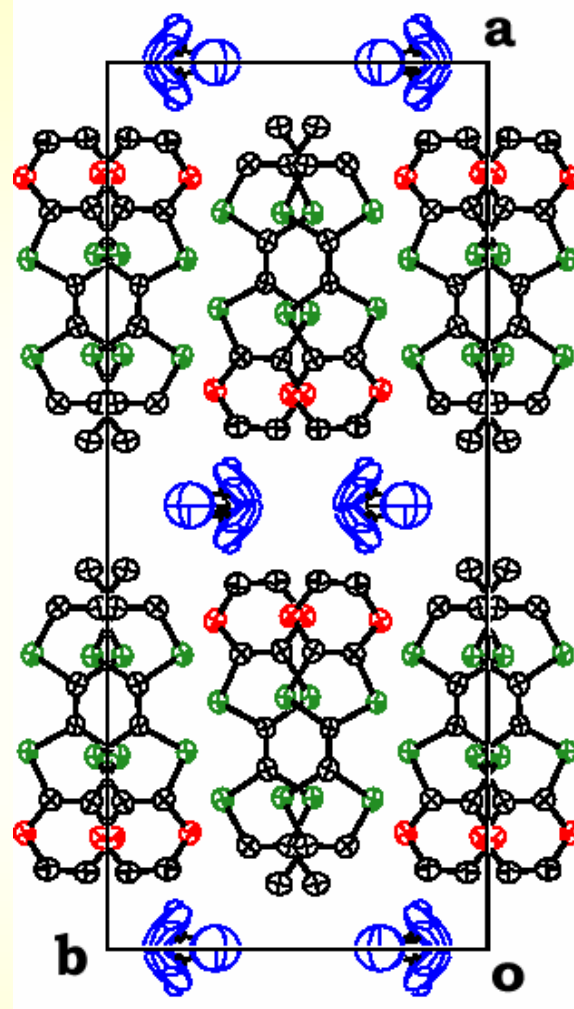
2:1 PF₆	σ_{rt} (S cm ⁻¹)
Black powder	3 (Semi.)
Dark green plates	29 (MI at 200 K)
Black plates	0.07 ↔ 4 (Semi.-Semi. at 303 K)

Crystal Structure of (MeEDO-TTF)₂X (X = BF₄, ClO₄)

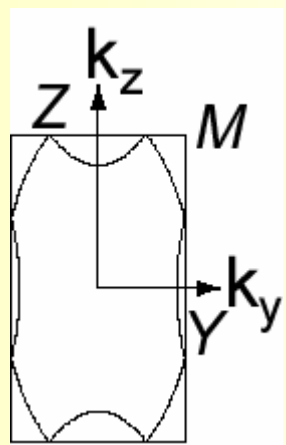
For X = BF₄



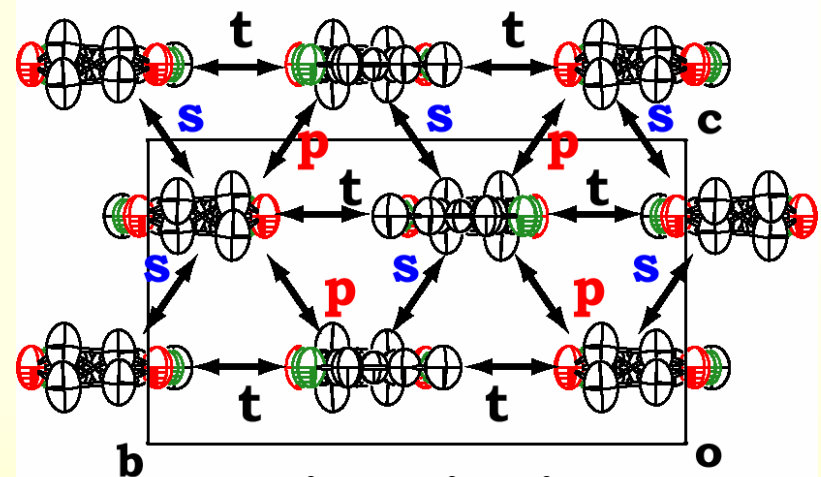
Orthorhombic
Cmcm
a = 28.752(2) Å
b = 12.369(1)
c = 6.969(1)
V = 2478.4(4) Å³
Z = 4
R = 5.7 %
(I_o > 2σ(I_o))
Goof = 1.044



c-axis projection



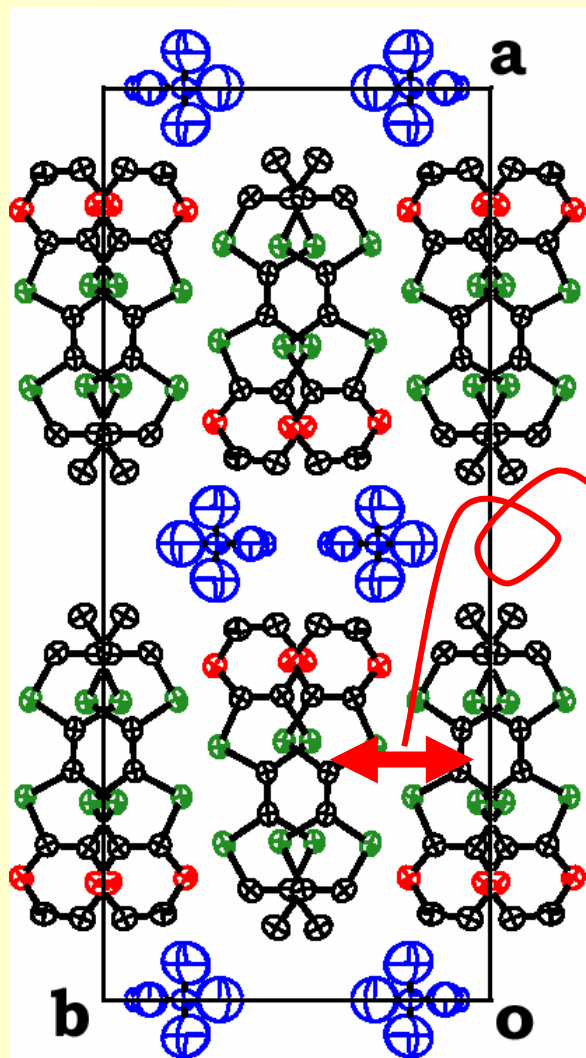
2D Fermi Surface
with weak intermol.
interactions



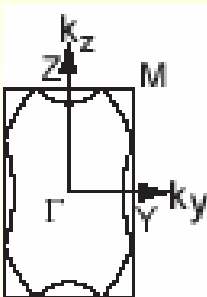
a-axis projection
t = 11.7, **p = 8.4**,
s = -5.1 × 10⁻³

Donor: Head-to-Head
(parallel)
Anion: Disordered

(MeEDO-TTF)₂PF₆: Semiconductor-Semiconductor

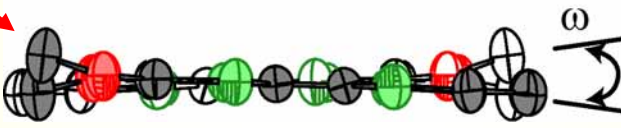


H-phase

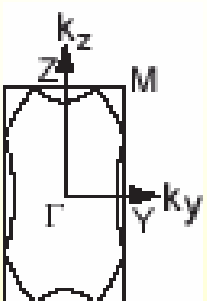


Nearly Localized Charge-order

$$\omega = 0^\circ$$

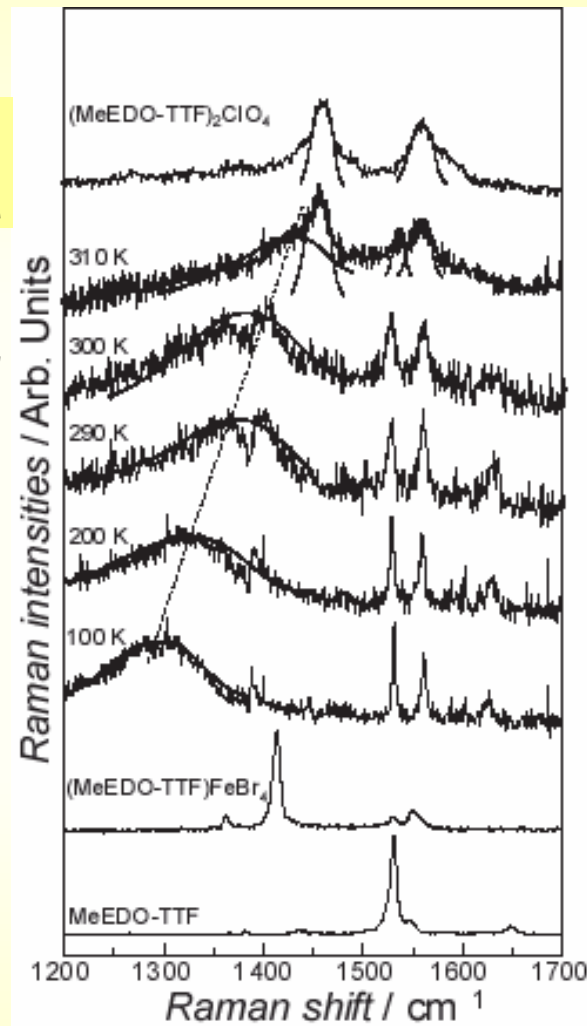


L-phase



Definitive Charge-order

$$\omega \approx 4^\circ$$



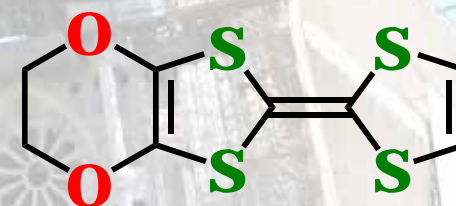
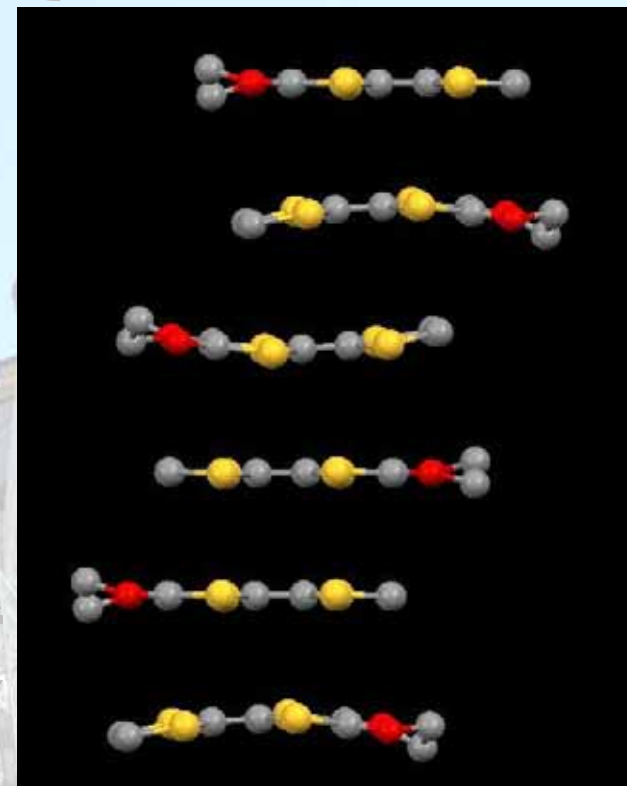
Black Plate H-phase
isostructural with
metallic BF₄ & ClO₄

V/t

Area of Conducting Layer (Å²)
Stable BF₄ ClO₄ PF₆ Semi-
metal 86.19 86.41 | 88.07 conductor

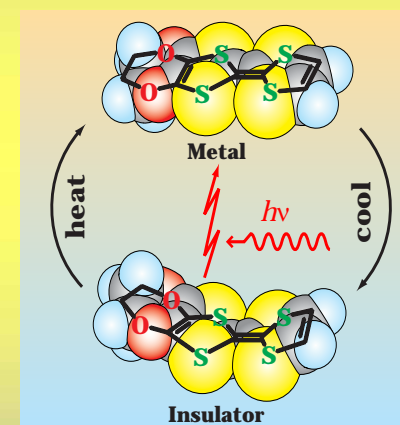
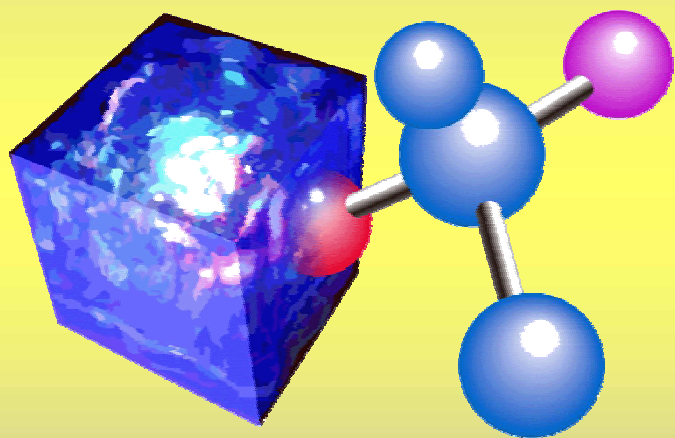
有機導電体における 分子自由度

- 格子点 \neq 点
形状・大きさ・機能性
形状変化が可能
- 新たな機能性物質
多重不安定性
外場敏感相転移物質
光誘起相転移物質
開始時刻の制御
非平衡状態の研究



低温物質科学研究センター

Research Center for Low Temperature and Materials Sciences



分子性材料開拓・解析研究分野

Division of Molecular Materials Science